EDGE LOCALIZED MODE CONTROL IN DIII-D USING MAGNETIC PERTURBATION-INDUCED PEDESTAL TRANSPORT CHANGES

by
R.A. MOYER, T.E. EVANS, K.H. BURRELL, T.H. OSBORNE,
M.E. FENSTERMACHER, J.A. BOEDO, E.J. DOYLE,
G.R. MCKEE, T.L. RHODES, D.L. RUDAKOV, G. WANG,
J.G. WATKINS, L. ZENG, P. THOMAS, M. BECOULET,
I. JOSEPH, S. KASILOV, G.D. PORTER, A. RUNOV,
M.J. SCHAFFER, R. SCHNEIDER, and P.B. SNYDER

JULY 2006

GENERAL ATOMICS

DISCLAIMER

GA–A25500

EDGE LOCALIZED MODE CONTROL IN DIII-D USING MAGNETIC PERTURBATION-INDUCED PEDESTAL TRANSPORT CHANGES

by

R.A. MOYER,* T.E. EVANS, K.H. BURRELL, T.H. OSBORNE,
M.E. FENSTERMACHER,[†] J.A. BOEDO,* E.J. DOYLE,[‡]
G.R. MCKEE,[£] T.L. RHODES,[‡] D.L. RUDAKOV, G. WANG,[‡]
J.G. WATKINS,[§] L. ZENG,[‡] P. THOMAS,[¶] M. BECOULET,[¶]
I. JOSEPH, S. KASILOV,[ƒ] G.D. PORTER,[†] A. RUNOV,[ç]
M.J. SCHAFFER, R. SCHNEIDER,[¶] and P.B. SNYDER

*University of California-San Diego, La Jolla, California
[†]Lawrence Livermore National Laboratory, Livermore, California USA
[‡]University of California-Los Angeles, California USA
[£]University of Wisconsin-Madison, Madison, Wisconsin
[§]Sandia National Laboratories, Albuquerque, New Mexico USA
[¶]Association EURATOM-CEA, Cadarache, France
[ƒ]Kharkov Institute for Physics and Technology, Kharkov, Ukraine
[ç]Max Planck Institute, Greifswald, Germany

GENERAL ATOMICS

1. INTRODUCTION

Control of the impulsive power loading to the divertor target plates due to Type I ELMs remains a critical issue for ITER because this loading is expected to exceed the ablation limit for graphite, resulting in reduced divertor PFC lifetimes and concomitant plasma contamination by the ablated carbon [1]. In 2002, it was proposed that an edge resonant magnetic perturbation (RMP) of about 1 part in 10^4 of the toroidal magnetic field would enhance transport enough to reduce the pedestal pressure gradient ∇p^{TOT} below the threshold for Type I ELMs without destroying the H-mode edge transport barrier [2]. In 2004, this ELM control scheme was demonstrated in DIII-D with edge RMPs that suppressed the ELM energy and particle impulses to the divertor by factors of 5–8 without degrading core confinement in H-modes with moderate pedestal collisionality $v_e^* > 1$ [3,4] [Fig. 1(a)]. In 2005, these results were extended to ITER-relevant low collisionality $v_e^* \sim 0.1$, where Type I ELMs were eliminated for up to 18 energy confinement times, limited only by the I-coil pulse and plasma discharge durations [Fig. 1(a)] [5,6]. At both collisionalities, the resulting ELM-free H-modes were in steady-state with little impact on overall energy confinement, as shown by the H-mode confinement quality factor H98y2 in Fig. 1(a).
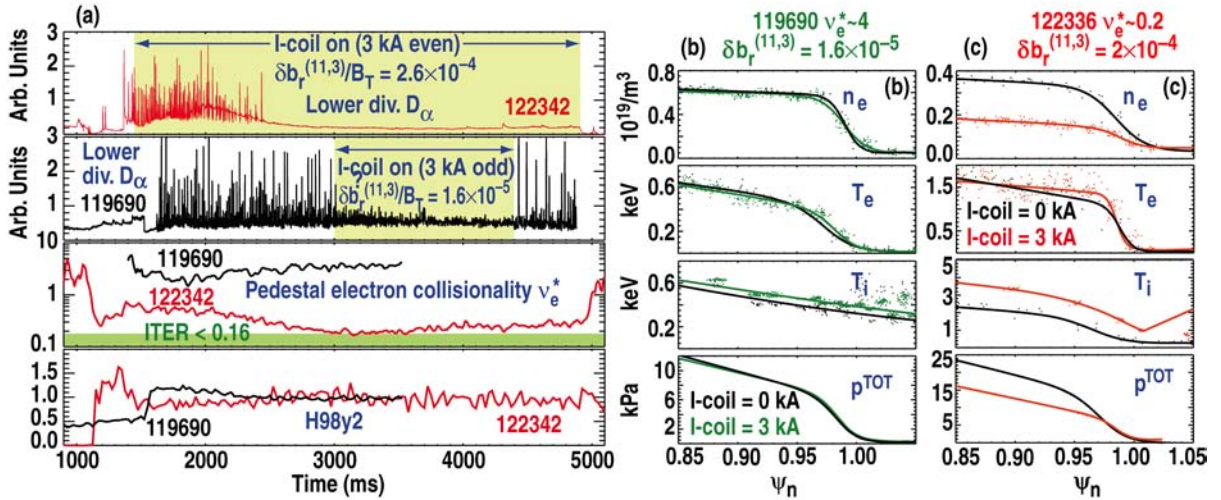

Fig. 1. (a) ELM suppression in (red) $v_e^* \sim 0.1$ and (black) $v_e^* > 1$ discharges, showing (top to bottom): divertor D_α in $v_e^* \sim 0.1$ and $v_e^* > 1$ discharges, pedestal electron collisionality v_e^*, and H98y2. The timing of the RMP pulse is indicated by the shaded areas in the D_α traces. Pedestal profile changes in (b) $v_e^* > 1$ and (c) $v_e^* \sim 0.1$ discharges, showing (top to bottom): electron density n_e, electron temperature T_e, ion temperature T_i, and total pressure p^{TOT}. The profiles just before the ELM (I-coil off) are shown in black. The pedestal profiles during the I-coil RMP pulses are shown in green ($v_e^* > 1$) and red ($v_e^* \sim 0.1$). The lines are fits to the experimental data, indicated by dots of the corresponding color.

2. PEDESTAL PROFILE CHANGES DURING RMP ELM SUPPRESSION

The pedestal profile changes during RMP ELM suppression are shown in Fig. 1(b) for moderate collisionality and in Fig. 1(c) for low collisionality. At $v_e^* > 1$ [Fig. 1(b)], the pedestal profiles averaged over the ELM-free phase have not changed significantly from the profiles just before an ELM without the RMP. In contrast, at $v_e^* \sim 0.1$ [Fig. 1(c)], ∇p^{TOT} drops significantly during the RMP ELM suppression phase, primarily due to a decrease in the pedestal electron density n_e. Changes in the T_e profile are relatively small at both collisionalities. Together, the large change in particle transport and lack of a large change in electron thermal transport appear to be inconsistent with expectations from stochastic layer transport models [6,7].

3. RMP-INDUCED CHANGES TO PEELING-BALLOONING STABILITY

Although the applied RMP suppresses Type I ELMs, the suppression mechanism does not always lower ∇p^{TOT}. For $v_e^* > 1$, the RMP-induced changes to ∇p^{TOT} are small and within the error bars in the profile measurements [Fig. 2(a)]. In contrast, at $v_e^* \sim 0.1$, the RMP changes the peak, width, and location of ∇p^{TOT}, each of which can alter peeling balloon (PB) stability [Fig. 2(b)]. Analysis of the linear stability of PB modes in the $v_e^* \sim 0.1$ discharges with the ELITE code [8] confirms that the observed ∇p^{TOT} changes move the pedestal into the linearly stable portion of the PB stability space as intended [Fig. 2(c)] [9]. Because the ∇p^{TOT} changes at $v_e^* \sim 0.1$ scale with the RMP amplitude [5,6], the H-mode pedestal can be pushed deep into the linearly stable portion of the operating space with increasing RMP amplitude [green ovals in Fig. 2(c)], suggesting that the ELM control can be tuned by varying the externally applied field.
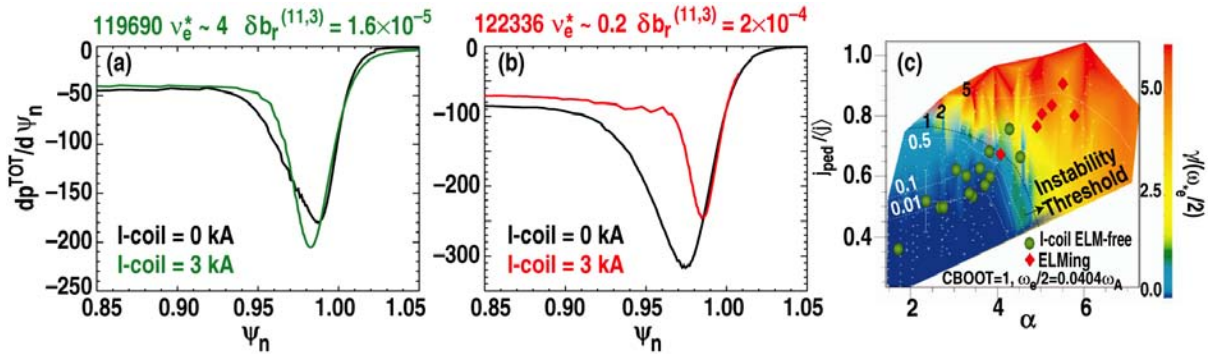

Fig. 2. Comparison of the ∇p^{TOT} change in (a) $v_e^* > 1$ and (b) $v_e^* \sim 0.1$ H-modes with RMP-induced ELM suppression. ∇p^{TOT} just before the ELMs without the RMP is shown in black; ∇p^{TOT} during RMP is shown in green ($v_e^* > 1$) and red ($v_e^* \sim 0.1$), respectively. (c) Contour plot of the normalized linear growth rate for PB modes in ($j_{ped}/\langle j \rangle, \alpha$) space, where j_{ped} is the peak toroidal current in the pedestal, and α is proportional to ∇p^{TOT}. ELMing discharges are shown with red diamonds; RMP ELM-suppressed discharges are indicated by green ovals.

4. RMP-INDUCED PEDESTAL TRANSPORT CHANGES

The difference between the measured profile changes and expectations from stochastic transport theory suggest that mechanisms other than parallel transport along chaotic field lines replace the ELM-induced transport to maintain the steady-state H-mode. At $\nu_e^* > 1$, the ELM-induced transport appears to be replaced by transport associated with small bursts in D_α [Fig. 1(a) and green D_α trace in Fig. 2(a)]. These oscillations are correlated with bursts of magnetic fluctuations $\dot{B}$ in the edge that drive smaller but more continuous loss of pedestal stored energy, as indicated by the decreases in stored energy and pedestal SXR emissivity in Fig. 3(a) [4]. These events are reminiscent of Type II ELMs in some discharges, and are correlated with an increase in the size and frequency of intermittent transport events at the last closed flux surface [9].
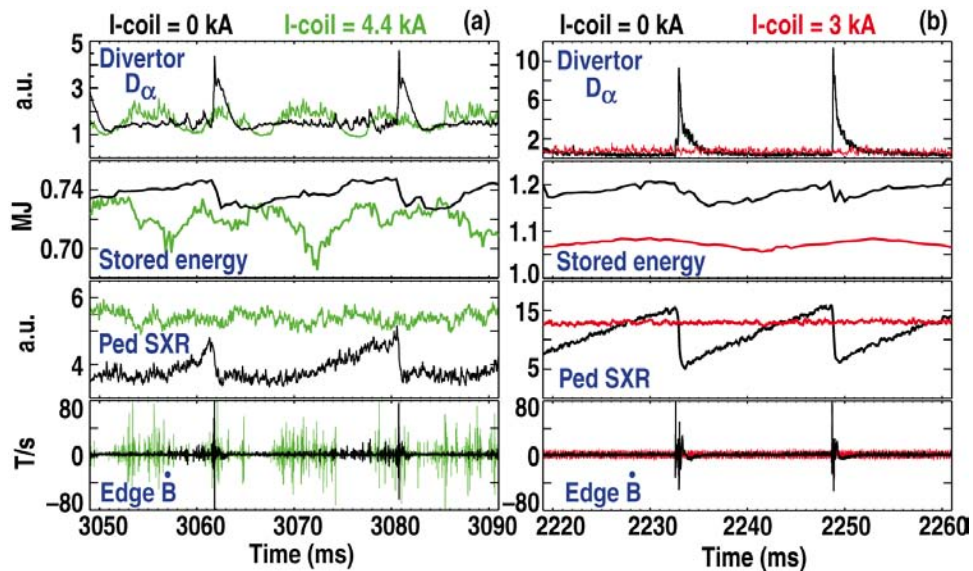

Fig. 3. (a) Transport events in $\nu_e^* > 1$ discharges during RMP ELM suppression (green) and an I-coil off reference discharge (black), showing top to bottom: D_α, stored energy, pedestal SXR emissivity, and edge magnetic fluctuations $\dot{B}$. (b) Corresponding signals in $\nu_e^* \sim 0.1$ discharges during RMP ELM suppression (red) and an I-coil off reference discharge (black). The quiescent character of the ELM suppressed phase at low collisionality (red) is evident in all the signals.

In Fig. 4, the density fluctuation changes measured by homodyne reflectometry near $\psi_n \sim 0.98$ are shown for both collisionalities. The divertor D_α trace is shown for reference in Fig. 4(a) and (d); the rms amplitude of density fluctuations $\tilde{n}_{rms}$ is shown in Fig. 4(b) and (e); and the time dependence of the density fluctuation amplitude spectra are shown as color contour plots in Fig. 4(c) and (f). At $\nu_e^* > 1$, $\tilde{n}_{rms}$ during ELM suppression [Fig. 4(b)] remains essentially constant during the ELM-suppressed phase (after 3000 ms). In contrast, at $\nu_e^* \sim 0.1$, $\tilde{n}_{rms}$ loses the bursty character during the ELMing phase (before 2000 ms) and

increases by a factor of 3 [Fig. 4(e)] over the level between the ELMs before the RMP pulse. This increase in broadband density fluctuations in the pedestal occurs without a corresponding increase in edge magnetic fluctuations [Fig. 3(b)].
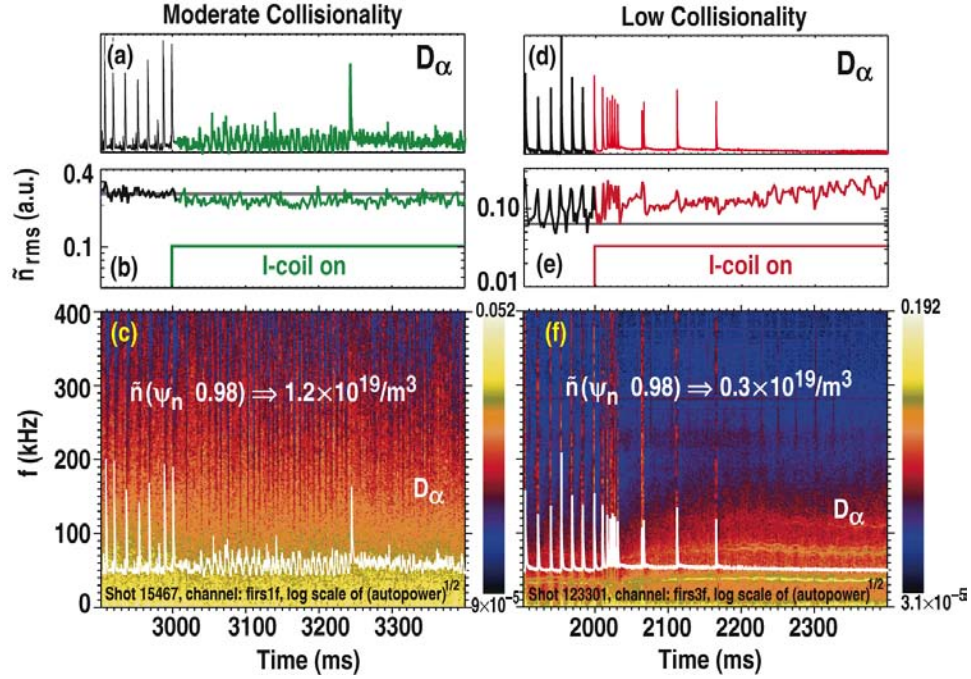

Fig. 4. (a) Divertor D_α, (b) $\tilde{n}_{rms}$ at $\psi_n = 0.98$, and (c) color contour plot of the $\tilde{n}$ amplitude spectrum versus time across the RMP turn on for $\nu_e^* > 1$. (d) Divertor D_α, (e) $\tilde{n}_{rms}$ at $\psi_n = 0.98$, and (f) color contour plot of the $\tilde{n}$ amplitude spectrum versus time across the RMP turn on for $\nu_e^* \sim 0.1$. Divertor D_α signal (white) is overlaid on the $\tilde{n}$ amplitude spectra for reference.

5. CONCLUSIONS

Edge RMPs suppress large ELMs over a range of pedestal conditions in DIII-D. At $v_e^* > 1$, the ELMs are replaced by small transport events that produce smaller, quasi-continuous pedestal energy losses. At $v_e^* \sim 0.1$, the pedestal during the ELM-suppressed phase is quiescent, but broadband pedestal density fluctuations increase, suggesting that ELM-induced transport may be replaced in part by increased electrostatic fluctuation-driven transport in the low collisionality discharges. This increase may account for the large changes in particle transport seen in the low collisionality ELM-suppressed phase, but not predicted by stochastic layer transport theory.

REFERENCES

[1] G. Federici, A. Loarte, G. Strohmayer, Plasma Phys. Control. Fusion **45**, 1523 (2003).

[2] T.E. Evans, R. A. Moyer, and P. Monat, Phys, Plasmas **9**, 4957 (2002).

[3] T.E. Evans, R.A. Moyer, P.R. Thomas, et al., Phys. Rev. Lett. **92**, 235003-1 (2004).

[4] R.A. Moyer, T.E. Evans, T.H. Osborne, et al., Phys. Plasmas **12**, 056119 (2005).

[5] K.H. Burrell, et al., Plasma Phys. Control. Fusion **47**, B37 (2005).

[6] T.E. Evans, R.A. Moyer, K.H Burrell, et al., Nature Physics **2**, 419 (2006).

[7] I. Joseph, et al., in press: J. Nucl. Mater. 2006.

[8] P.B. Snyder, H.R. Wilson, J.R. Ferron, et al., Nucl. Fusion **44**, 320 (2004).

[9] J.A. Boedo et al., this meeting (2006).

ACKNOWLEDGMENTS